E. Poutou · G. Krinner · C. Genthon · N. de Noblet-Ducoudré

Role of soil freezing in future boreal climate change

Abstract We introduced a simple scheme of soil freezing in the LMDz3.3 atmospheric general circulation model (AGCM) to examine the potential effects of this parameterization on simulated future boreal climate change. In this multi-layer soil scheme, soil heat capacity and conductivity are dependent on soil water content, and a parameterization of the thermal and hydrological effects of water phase changes is included. The impact of these new features is evaluated against observations. By comparing present-day and $2\times CO_2$ AGCM simulations both with and without the parameterization of soil freezing the role of soil freezing in climate change is analysed. Soil freezing does not have significant global impacts, but regional effects on simulated climate and climate change are important. In present-day conditions, hydrological effects due to freezing lead to dryer summers. In $2\times CO_2$ climate, thermal effects due to freeze/thaw cycles are more pronounced and contribute to enhance the expected future overall winter warming. Impact of soil freezing on climate sensitivity is not uniform: the annual mean warming is amplified in North America ($+15\%$) and Central Siberia ($+36\%$) whereas it is reduced in Eastern Siberia (-23%). Nevertheless, all boreal lands undergo a strong attenuation of the warming during summertime. In agreement with some previous studies, these results indicate once more that soil freezing effects are significant on regional boreal climate. But this study also demonstrates its importance on regional boreal climate change and thus the necessity
to include soil freezing in regional climate change predictions.

E. Poutou · G. Krinner (✉) · C. Genthon
Laboratoire de Glaciologie et Géophysique
de l'Environnement, CNRS-UJF, 54 rue Molière,
BP 96, St. Martin d'Hères, France
E-mail: krinner@lgge.obs.ujf-grenoble.fr
Tel.: +33-476-824241
Fax: +33-476-824201

N. de Noblet-Ducoudré
Laboratoire des Sciences du Climat et de l'Environnement,
CEA-CNRS, Gif-sur-Yvette, France

1 Introduction

In boreal regions, low temperatures lead to the formation of frozen ground and permafrost zones, this latter currently underlying nearly one fourth of the exposed land area of the Northern Hemisphere (Zhang et al. 1999). The presence of frozen ground plays an important role in the polar ecology. The main effect of seasonal soil freezing and thawing is that it delays the summer warming and the winter cooling of the surface. It also affects the soil hydrology by impeding soil drainage and creating high soil moisture contents in the seasonally thawed upper soil layer, called the active layer. Under anthropogenic warming at high latitudes, several studies suggest a thinning or a reduction of permafrost and frozen ground areas (Nelson and Anisimov 1993; Anisimov and Nelson 1997; Anisimov et al. 1997; Demchenko et al. 2001; Smith and Burgess 1999). Such changes could have severe impacts on northern ecosystems. In particular, a thicker active layer, where most exchanges of energy, moisture and gases occur, could destabilize geomorphical, hydrological and biological processes (Nelson and Anisimov 1993; Weller et al. 1995). In some regions, it could also trigger the release of significant amounts of greenhouse gases to the atmosphere (Fukuda 1994; Michaelson et al. 1996; Goulden et al. 1998).

However, the linkages between frozen grounds and climate remain insufficiently studied and their effects on climate still poorly represented in land surface schemes. Recently, the project for intercomparison of land surface parameterization schemes (PILPS) (Henderson-Sellers et al. 1993, 1995) between soil-vegetation-atmosphere transfer (SVAT) schemes has underlined the importance of modelling cold-climate land surface processes

(Schlosser et al. 2000; Bowling et al. 2003). For example, Schlosser et al. (2000) have shown that the parameterization of frozen soil (or lack of such a parameterization) was a cause for considerable error in predicted soil moisture, which, in turn, was related to disparity in predicted surface fluxes. The treatment of soil freezing was also shown to have long-term effects on model variability. Efforts have been made in modelling thermal and hydrologic characteristics of frozen soils (Fox 1992; Koren et al. 1999), the freezing front depth (Gel'fan 1989) and in representing and validating soil freezing (Cherkauer and Lettenmaier 1999). But the non-linearity and complexity of frozen soil physics, particularly the coupling of thermal and hydrological processes, complicate its inclusion into more sophisticated models like the SVAT schemes and general circulation models (GCMs).

The following studies are few examples of the inclusion of soil freezing in climate models. Smirnova et al. (2000) have recently included in the mesoscale analysis and prediction system (MAPS) (a coupled atmospheric/land surface model) the parameterizations of processes in frozen grounds. Their comparisons with observed data from Valdai, Russia, show that the MAPS 1-D soil-vegetation-snow model provides accurate simulations and that especially runoff is improved during the spring melting season. Viterbo et al. (1999) also improved the European centre for medium-range weather forecasts (ECMWF) model by including the process of soil moisture freezing. Compared to the previous ECMWF version (Viterbo and Beljaars 1995), this has contributed to eliminate the systematic 2 m air temperature biases for winter and to make the soil temperature evolution more realistic. Improvements of atmospheric simulations for high-latitude regions were also found by Cox et al. (1999) when including soil water phase changes in the UK meteorological office surface exchange scheme (MOSES) SVAT coupled to a climate model. Boone et al. (2000) also obtained more realistic surface fluxes with the inclusion of soil ice into the interactions between the soil, biosphere, and atmosphere (ISBA) SVAT scheme.

These studies highlight the impact of soil freezing parameterizations in climate simulations. Therefore, climate change could also be influenced by this process, but as far as we know, this has never been studied.

Nevertheless, some sensitivity experiments to the representation of other parameters (such as the snow cover, the albedo) have shown some changes in the climate response to specific forcing conditions. For example, Cox et al. (1999) noted more significant reductions in available soil moisture and evaporation under $2\times CO_2$ conditions when using MOSES (including soil water phase changes), compared to the previous UKMO scheme. Different prescribed hot desert albedos have also been tested by Bonfils et al. (2001) who demonstrated their impacts on the simulated mid-Holocene summer monsoon change in northern Africa. They found larger changes when the albedo values are the lowest. Furthermore, according to Douville and Royer (1996), the Asian monsoon activity is significantly weakened when a larger Eurasian snow thickness in spring is prescribed in the Météo-France model.

These studies demonstrate several climatic feedback mechanisms induced by changes in albedo (Bonfils et al. 2001), snow cover (Douville and Royer 1996) and soil water phases (Cox et al. 1999) in models. But the impact of soil freezing alone on climate changes has not been yet studied. Hence, in this paper we are motivated by the sensitivity of a simulated future climate change to soil freezing. Renssen et al. (2000) have already shown that incorporating a simple parameterization of permafrost in a Younger Dryas climate simulation substantially improved the agreement with paleodata. They also concluded that permafrost could have played a more important role than usually expected in paleoclimates and especially during cold periods.

In this study, an atmospheric general circulation model (AGCM) is used to quantify the effects of soil freezing parameterization on simulated climate and climate change. The aims are (a) to introduce a soil freezing scheme consistent with an AGCM, (b) to understand how the inclusion of soil freezing can modify the high latitude climate response and (c) to assess the importance of soil freezing in predictions of boreal climate change. We first describe the soil freezing scheme incorporated in the LMDz3.3 AGCM, a model version adjusted by Krinner et al. (1997) to improve model performance over polar regions. This soil freezing scheme is evaluated in stand-alone simulations using PILPS 2(d) observational data (Vinnikov et al. 1996; Schlosser et al. 1997). We then focus on the potential impacts of soil freezing processes on present-day and on $2\times CO_2$ climate. Finally, we discuss the climate change sensitivity to soil freezing.

2 Methods

2.1 Soil freezing scheme

The baseline version of the LMDz3.3 AGCM has a rather simple soil scheme. Soil humidity is treated by a bucket scheme with a depth of 1 m and a field capacity of $f = 0.15$ m^3 water m^{-3} soil. Soil temperatures are calculated with a multilevel heat conduction scheme. Generally, 11 layers are used, the vertical discretisation being calculated as a geometric series with layer thickness increasing towards the deeper layers. The total soil depth is 15 m. The equilibrium time scale of the deepest soil layer (that is, the e-folding time of the deepest layer to adjust to an instantaneous surface climate change) is about 10 years. In the baseline version of the AGCM, soil heat capacity and conductivity are prescribed as fixed values, independent on soil type or water content.

This scheme has been modified for the experiments used here. In all simulations (with and without soil

freezing), soil heat capacity and conductivity are variable, depending on soil water, and, for simulations with soil freezing, ice content. Depending on the temperature of each thermal soil layer, the moisture is either diagnosed as ice or liquid water when soil freezing is taken into account (otherwise, only liquid water is present).

Following Lunardini (1988) and Bonan (1996), volumetric heat capacity c (in J kg^{-1} K^{-1}) is then calculated for each soil layer as a function of (frozen or liquid) soil water content and temperature:

$$c = (1 - \theta_{sat})\rho_s c_s + \rho_w c_w \theta_w + \rho_i c_i \theta_i + \tilde{c} \qquad (1)$$

Here θ_{sat} is the maximum volumetric water content (set to 0.4); c_s is the specific dry soil heat capacity (in J m^{-3} K^{-1}); $c_{i/w}$ the specific water/ice heat capacity (in J m^{-3} K^{-1}); $\theta_{w/i}$ is the volumetric water/ice content; $\rho_{s/w/i}$ is the density of dry soil, water, and ice, respectively (in kg m^{-3}); and $\tilde{c}$ is an apparent heat capacity representing the latent heat release and uptake during water phase changes:

$$\tilde{c} = \frac{\theta \rho_w L}{2\Delta T} \qquad (2)$$

Here, L is the specific latent heat of fusion of water (in J kg^{-1}), and ΔT is the temperature interval around 0°C over which the phase change occurs (here, $\Delta T = 0.5°C$). Within this interval, the fraction of liquid water linearly increases from zero to one as temperature increases from $-\Delta T$ to $+\Delta T$ degrees Celsius. When soil freezing is not taken into account, $\tilde{c}$ is always zero. Similarly, θ is then simply the water (and not ice) content, and soil heat capacity does not depend on temperature. Otherwise, depending on the temperature of the soil level, the appropriate heat capacity (c_w, c_i, or a blended value within the transition interval) is used. As the soil hydrology is treated by a bucket model, soil moisture is supposed to be constant over the whole soil column. The treatment is somewhat more complicated when soil freezing is taken into account and soil temperature is below 0°C. In this case, we use the soil humidity that prevailed at the moment when the soil temperature at this level decreased below the freezing point. This is done in order to ensure energy conservation, in particular in Eq. 2, as the energy released in autumn, when soil temperatures fall below 0°C, must be exactly taken up again in springtime when the soil thaws.

Following Farouki (1981), heat conductivity k is calculated as a function of soil water and ice content:

$$k = (k_{sat} - k_{dry})\theta + k_{dry} \qquad (3)$$

Here k_{sat} is the conductivity of saturated soil, k_{dry} the conductivity of dry soil, and θ soil moisture. The saturated soil conductivity is calculated as

$$k_{sat} = k_s^{1-\theta_{sat}} k_i^{(1-f_l)\theta_{sat}} k_w^{f_l\theta_{sat}} \qquad (4)$$

where k_s, k_i and k_w are the conductivities of the soil solid, ice and water; and f_l is the fraction of the soil

water that is present in liquid state, varying linearly from zero to one over a temperature interval from $-\Delta T$ to $+\Delta T$. As stated before, the soil hydrology in LMDz3.3 is treated by a bucket scheme. Therefore, impact of soil freezing on soil hydrology can only be modelled in a fairly crude way. On local scales, the main hydrological effect of the presence of frozen ground is a reduction of water infiltration (Farouki 1981). Takata and Kimoto (2000) report that taking into account the impermeability of frozen soil to spring meltwater leads to increase runoff of meltwater during spring (instead of soil infiltration), thereby causing significantly reduced summer soil wetness and, consequently, higher summer surface temperatures over the boreal continents. Here, local infiltration reduction is represented in a very schematic way by scaling soil water infiltration with the fraction of unfrozen ground within the uppermost meter beneath the surface. That is, infiltration vanishes when the entire top meter of soil is frozen.

However, Cox et al. (1999) note that on spatial scales such as those of typical GCM resolution, heterogeneities in frozen soil and soil freezing hydraulic conductivity would allow surface runoff from frozen soil surface to infiltrate into the soil elsewhere in the same grid box. Moreover, large wetlands exist in the high northern latitudes, particularly in flat regions (Matthews and Fung 1987; Prigent et al. 2001). Fed by meltwater in spring, the wetlands prevent the surface runoff from being lost to the oceans. To represent this large-scale effect in the GCM, water that cannot infiltrate the soil, either because the soil is saturated or because of the presence of ice in the uppermost meter of the soil, is temporarily stocked in a runoff reservoir R that can simply be interpreted as stagnant surface water or "wetlands". This runoff reservoir does not directly interact with the atmosphere. It loses water immediately by soil infiltration as soon as the soil, through thawing or evaporation, can again accept water. Moreover, R loses water to the oceans with a prescribed time constant τ_R:

$$\frac{\partial R}{\partial t} = -\frac{R}{\tau_R} - T_{r \leftrightarrow s} \qquad (5)$$

Here $T_{r \leftrightarrow s}$ represents the immediate water mass exchange between the soil and the runoff reservoir as described above, while R/τ_R is the flux of water lost to the oceans. Similar to Krinner (2003), the runoff time constant τ_R is tentatively prescribed as a function of subgrid-scale topography. In mountainous regions (such as Eastern Siberia), τ_R is of the order of a day or so (that is, excess water is rapidly lost to the oceans), while over flat regions such as the Ob plains, it can reach up to about 200 days, which is similar to the remotely sensed temporal fraction of wetland inundation in flat boreal areas (Prigent et al. 2001). In order to test the new soil freezing scheme, this surface model can be run in off-line mode. In particular, off-line tests for the PILPS 2(d) site (Schlosser et al. 2000; Luo et al.

2003) are described in Sects. 2.2.1 and 3. Offline simulations have also been carried out to accelerate convergence towards the thermal soil equilibrium in our simulations (see Sect. 2.2.2).

2.2 Simulation set up

2.2.1 Stand-alone simulation

A main goal of the PILPS phase 2(d) experiment at Valdai, Russia, was to provide an opportunity to evaluate cold region land surface processes (Schlosser et al. 2000; Luo et al. 2003). Continuous atmospheric forcing data for 18 years (1966–1983) exist for this station situated at 57.6°N and 33.1°E (Vinnikov et al. 1996; Schlosser et al. 1997). For stand-alone tests of the modified parameterizations, the whole surface package of LMDz3.3 (that is, surface and boundary layer parameterizations, the latter being necessary for calculating the turbulent surface fluxes) has been extracted from the AGCM so that it can be forced by observed half-hourly meteorological data from Valdai.

We carried out two off-line simulations: one without, and one with soil freezing and with the runoff reservoir. The first 3 years of the simulations were discarded as spinup. The results reported in Sect. 3 therefore refer to the years 1969–1983.

2.2.2 AGCM simulations

The global atmospheric model used is LMDz3.3, with physical parameterizations described in Harzallah and Sadourny (1995). In the present study, a regular grid with 96 longitudes, 73 latitudes, and 19 vertical levels is used. Two simulations were conducted without the soil freezing process for present-day and $2\times CO_2$ climate (respectively referred to as PD-NF and $2\times CO_2$-NF). The two other simulations include soil freezing and are called: PD-F and $2\times CO_2$-F (see Table 1).

The AGCM LMDz3.3 was forced by observed sea surface conditions (SSC): sea ice concentrations and sea surface temperatures, derived from SSM/I satellite data over the period 1979–1995 (National Snow and Ice Data Center 1998) for present-day climate. Future simulations were carried out using prescribed monthly mean SSC calculated with the coupled-atmosphere-ocean model ECHAM4 AGCM (May and Roeckner 2001) and averaged over the period 2057–2099. As the control ECHAM4 AGCM SSC is judged fairly realistic (Roeckner et al. 1996), SSC relative to the period 2057–2099, are considered as a plausible future state. Moreover, we focus on the impact of varying model parameterizations on simulated climate change, not on the simulated climate change itself. Therefore, these future SSC were directly imposed in the model.

The concentrations of CO_2 were fixed at 330 ppm for present-day and 568 ppm for future climate. The value of 568 ppm, corresponding to twice of the preindustrial

Table 1 Simulation characteristics

Experiment	Soil freezing	CO$_2$ (ppm)
PD–NF	No	330
2×CO$_2$–NF	No	568
PD–F	Yes	330
2×CO$_2$–F	Yes	568

concentration is the average over the period 2057–2099, calculated with the results from the experiment GHG[1] realized by Roeckner et al. (1999). This choice is then consistent with the future SSC mentioned above.

All four simulations were performed for near equilibrium conditions during 30 years. Transient climate change is not modelled here. The periods considered represent the second halves of the twentieth and twenty-first centuries. The soil scheme is the slowest simulated part of the climate system in the model. To reach equilibrium without running the AGCM LMDz3.3 over more than 50 years, the model was iteratively spun up: 1-year AGCM simulations with future CO_2 levels and SSC were alternated with 20-years off-line simulations with the AGCM soil scheme forced by atmospheric conditions obtained with the preceding AGCM run. Three iterations were computed for the soil scheme, allowing the deep soil temperature to reach equilibrium with the climate of the second half of the twenty-first century.

The aim of this paper is to investigate the role of permafrost and seasonal soil freezing in climate change in the light of their impact on surface temperatures and diurnal cycle, precipitation, evaporation, soil moisture, snow cover and latent and sensible surface heat fluxes. The analysis focuses on the Northern Hemisphere extratropical climate, as this is where soil freezing mainly occurs. To clarify the discussion, boreal lands are divided into three regions: North America (165°W–55°W; 50°N–80°N), Central Siberia (30°E–120°E; 50°N–80°N) and Eastern Siberia (120°E–180°E; 50°N–80°N).

3 Results from a stand-alone simulation at Valdai (Russia)

At Valdai, continuous soil temperature measurements at 20 cm depth exist for the years 1971–1983. Figure 1 displays the simulated and observed soil temperatures at 20 cm depth for these years.

When soil freezing is taken into account, the annual soil temperature amplitude is clearly diminished, and much closer to the observations. During the warm seasons, soil thaw consumes latent energy that would otherwise be used for heating the soil, while in winter, the opposite process prevents the soil from cooling too

---

[1]Here, the forcing is due to changing atmospheric concentrations of CO_2 and other well-mixed greenhouse gases.
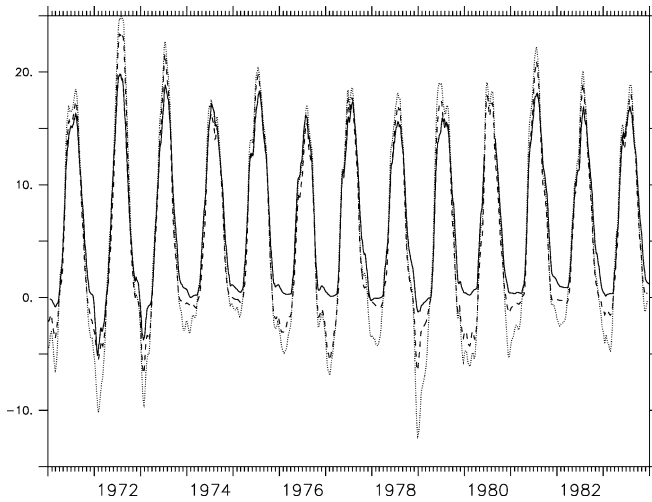
Fig. 1 Observed (*continuous line*) and simulated (*dotted* without soil freezing; *dashed* with soil freezing) soil temperatures in degree centrigrade at 20 cm below the ground at Valdai

much. During several winters (for example 1981–1982), the soil temperature at 20 cm depth remains fairly close to 0°C, indicating that the process of latent heat release in the soil prevents further cooling. However, although the simulation in which soil freezing is taken into account is more realistic than the control simulation without soil freezing, the annual soil temperature amplitude is still slightly overestimated. This is probably due to an inadequate soil thermal conductivity and/or soil heat capacity. Thus, active layer thickness in permafrost regions might be overestimated with this model.

Figure 2 displays the simulated soil moisture content of the uppermost meter for the years 1981–1983 (the other years are very similar). The impact of the soil freezing on the simulated soil moisture at Valdai is weak. This behaviour is expected, given the results of the
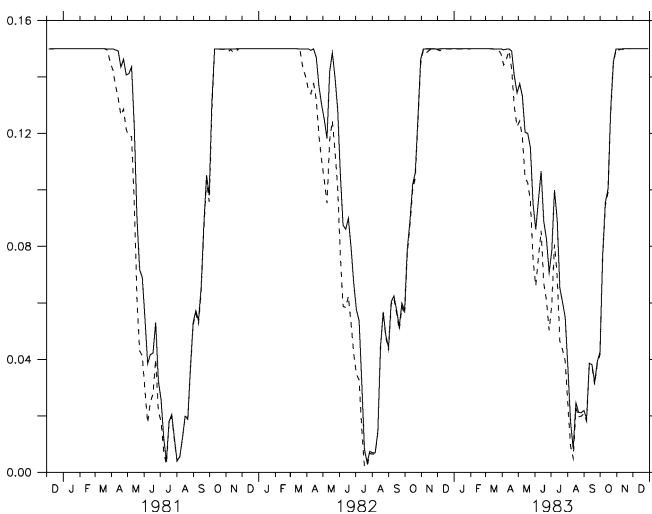

Fig. 2 Simulated soil moisture in the uppermost meter (in $m^3 \ m^{-3}$) for 1981–1983 at Valdai. *Continuous line* with soil freezing; *dashed line* without soil freezing

PILPS 2(d) model intercomparison exercise at Valdai reported by Luo et al. (2003). These authors report that, because of high soil water content during winter and because soil thaw occurs early at Valdai, the influence of frozen soil on infiltration is weak in the observations at Valdai, and insignificant in the models they analysed. Therefore, the results for the off-line simulations at Valdai cannot be used to validate the parameterizations of the hydrologic impact of soil freezing. However, as will be shown later, the ISLSCP (Meeson et al. 1995) and the R-ArCticNET (Lammers et al. 2000) dataset, suggest that large-scale soil humidity and river discharge are better simulated by the AGCM when soil freezing is taken into account.

4 AGCM results for present-day climate

The paper only focuses on patterns that are statistically significant at the level 95% for seasonal means and at 90% for annual means, based upon a student-test: only these patterns are discussed in the text. Seasonal means refer to winter (December–February), spring (March–May), summer (June–August) and autumn (September–November).

4.1 Impact of soil freezing on present-day climate

4.1.1 Soil hydrology

As mentioned in the introduction, the presence of ice in the soil limits the water infiltration into the deep soil levels (Farouki 1981). Accounting for soil freezing leads to a strong decrease in annual mean precipitation and soil moisture, the most striking effects occurring during summertime (Fig. 3). All seasons are dryer over North-West Canada, over a large part of Siberia and around the Baikal lake (between −60 and −73% of water in the soil). The sensitivity of soil moisture has been previously illustrated by Waelbroeck (1993) when validating a climate-soil processes approach in permafrost for the station Barrow, in Alaska.

Compared to PD-NF experiment, precipitations are reduced by about 0.5 mm day^{-1} in annual mean in PD-F, leading to large losses in regions characterised by weak precipitation in control climate conditions. For example, soil freezing implies a −20% reduction in Eastern Siberia and up to −35% around the Baikal lake during summertime. Decreasing precipitation occurs in spring when soil starts to thaw. Indeed solar energy is in that case used to melt soil ice and does not participate to the evaporation of available water at the surface as it does in the PD-NF simulation. When the top 1 m of the soil is frozen, the meltwater of snow cover goes directly into the oceans, reducing the soil evaporation in the following summer. Consequently, local recycling of precipitation is reduced and dryness effects are, once more, well marked in summer as shown on Fig. 3.
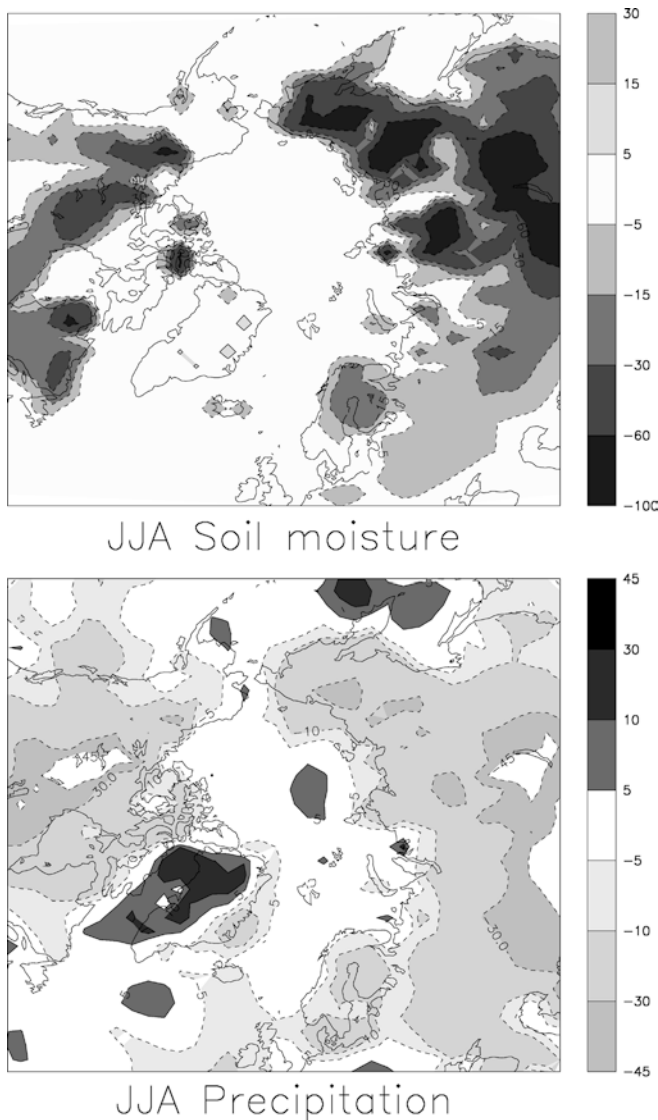
JJA Soil moisture

JJA Precipitation

Fig. 3 Changes in summer soil moisture and precipitation induced by soil freezing under present-day conditions. Soil moisture differences between PD-F and PD-NF experiments are given in percent of saturation. Differences in precipitation are in percent relative to the PD-NF run
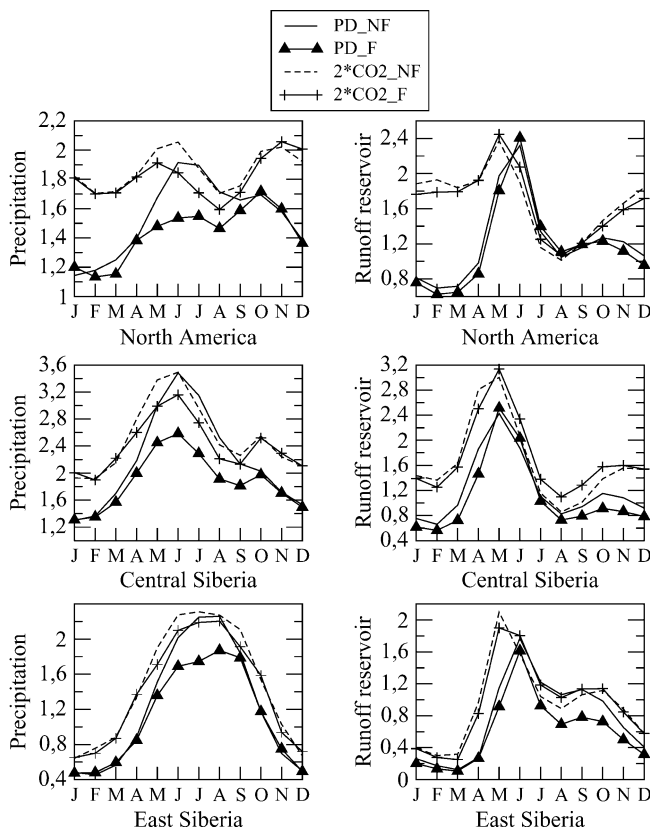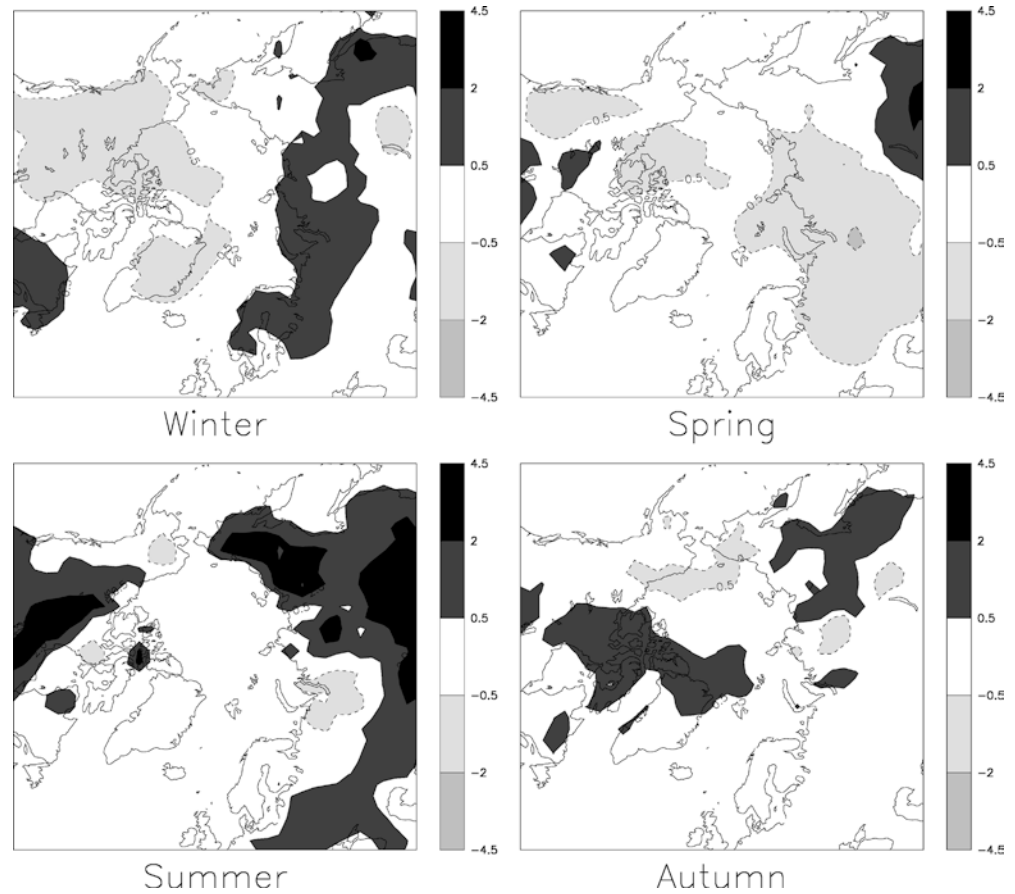
4.1.2 Soil surface temperatures

Soil freezing is a regulator of the soil thermal budget, by delaying the soil warming during melting season and by delaying the soil cooling during freezing season. Figure 4 shows the difference in surface temperatures between PD-F and PD-NF simulations in seasonal means, these patterns being stronger than those obtained in annual mean. A surface cooling effect appears during springtime over all Siberia and is less spread in North America. Indeed, thawing of frozen soil that is starting in April or May for the coldest regions, requires a large amount of energy (1 cm of frozen ground containing 20% of water needs 5.3×10^5 J m^{-2} to melt). This energy is taken mainly from the solar downward radiation,

delaying spring surface warming compared to the PD-NF simulation. The opposite effect, characterised by a release of energy during the freezing period in autumn, can be seen over the Baffin Land, the Canadian archipelago and around the Hudson Bay.

However, the reported effect of soil freezing on soil hydrology deviates from that behaviour. Summer is marked by a strong warming (between $+2$ and $+4$ K) in the PD-F simulation, whereas one could have expected a continuation of the thermal effect begun in spring. As mentioned before, the hydrological parameters such as precipitation and soil moisture exhibit a maximum of dryness in the PD-F experiment in all studied boreal regions. Over the three regions studied, this is clearly illustrated by seasonal variations of precipitation and runoff reservoir on Fig. 5, and by variations of soil moisture and snow cover on Fig. 6. Maximum of dryness comes from the fact that the modelled soil infiltration is limited by the presence of frozen ground, as suggested by Farouki (1981). In spring, the meltwater cannot infiltrate the soil straightaway and is stocked inside the runoff reservoir (which thus exhibits a maximum, Fig. 5) until it discharges into the oceans and seas, or returns to the soil when the soil is thawing. The flat plains of the West Canada, Central Alaska, Ob and Ienissei basins are characterised by a runoff time scale varying between 40 and 70 days. But even in the case of a long water storage, in summer, most of the meltwater has disappeared to the seas. Water transfer from the runoff reservoir (less than 1 cm) to the soil (when this latter is again able to accept water after thawing) is not enough to increase soil moisture (illustrated on Fig. 6) in summertime. Soil moisture reaches minimum value in August (in North America and Central Siberia) and a month before in Eastern Siberia (around -27%). This dryness implies a smaller rate of evaporation, also observed in the Bowen ratio (latent heat over sensible heat surface flux) leading to warmer surface conditions. As a large fraction of precipitation in these regions is due to local recycling of evaporation, the reduced evaporation rates yield to a general decrease in simulated precipitation (-20% in July). This represents a positive feedback on the soil dryness. The strong response of the dry soil has also been seen through the diurnal cycle of surface temperatures (not represented). A strong difference in the diurnal cycle of the two present-day simulations well appears in summer: accounting for soil freezing induces both an increase of the maximum (between 2.5 and 4.5 K) and a decrease of the minimum (down to -4 K) surface temperatures in the mean diurnal cycle. Thus, soil freezing leads to dryer soils, with reduced thermal inertia. The thermal effect of frozen ground discussed for the interseasons (latent heat release and uptake) alternates with an important hydrological effect, which raises surface temperatures during summertime.

Furthermore, on Fig. 4, the winter thermal effect due to freezing (and inducing warmer surface temperatures) is not present over all boreal lands. On the contrary,

Fig. 4 Differences in seasonal mean surface temperatures (K) between PD-F and PD-NF experiments. Winter stands for monthly averages over December, January and February; spring for March, April, and May; summer for June, July and August; autumn for September, October and November

Northwestern Canada and Alaska are characterised by cooler surface temperatures in PD-F experiment. This may be understood by looking at atmospheric transport and at the snow cover. Winter climate in polar regions is particularly strongly conditioned by the atmospheric circulation because of the lack of local heat generation. Surface temperature changes between PD-F and PD-NF simulations are coherent with changes in sea level pressure changes, shown on Fig. 7. Warmer air coming from the Atlantic ocean is advected over Siberia, north of which a depression occurs (up to −2 mbar). Polar cold air is shifted southward over North America and induces a slight cooling there (−0.5 K).

Regional differences in snow cover and in the induced thermoinsulation effect can also be invoked. Figure 6 shows a higher snow cover in Eastern and Central Siberia (80 cm water equivalent at maximum) than in North America (70 cm water equivalent at maximum). During autumn, the formation of frozen ground is delayed in all Siberia because of an earlier presence of snow cover than in North America, which isolates the top soil and prevents the downward propagation of the

Fig. 5 Seasonal cycle of precipitation (mm day^{-1}) and runoff reservoir (cm) in the four experiments over the studied regions: North America (165–55°W; 50–80°N), Central Siberia (30–120°E; 50–80°N) and Eastern Siberia (120–180°E; 50–80°N)
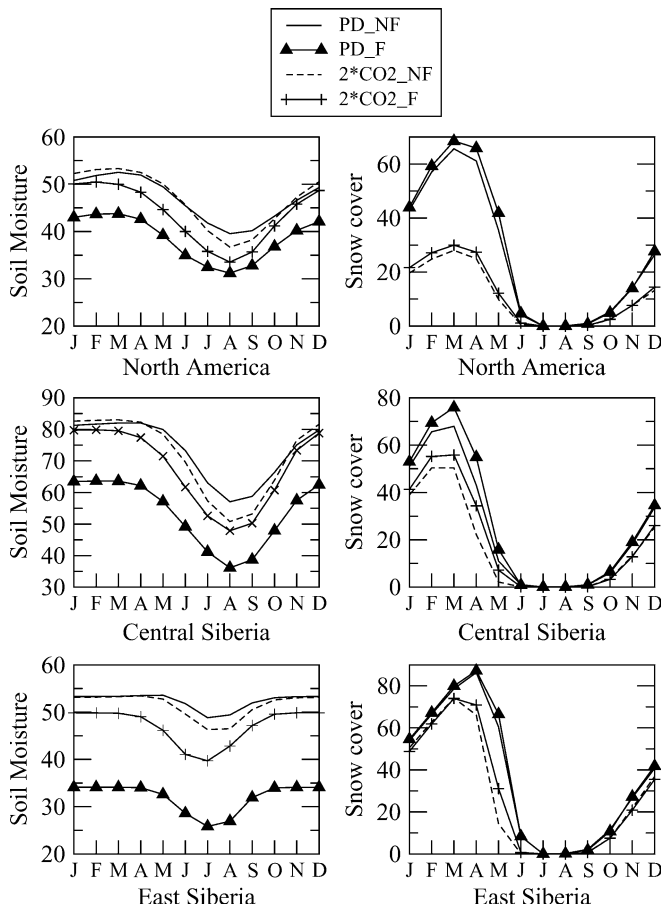
Fig. 6 Seasonal cycle of soil moisture (%) and snow cover (mm equivalent water) in the four experiments over the three studied regions

cold wave. Thus, the freezing process extends into winter, leading to warmer surface temperatures than in North America, in the PD-F experiment. In North America, freezing starts in autumn and snow cover is lower than in Siberia. Consequently, the top soil is more affected by the cold air temperatures at this period and the cold wave can propagate easily into the deepest layers due to the high conductivity of ice.

4.2 Improvements in the simulated climate

The introduction has underlined some beneficial effects of the inclusion of soil water phase changes in simulated present-day climate. Figure 8 gives the errors in 2 m air temperatures simulated by LMDz3.3 in PD-F and in PD-NF experiments relative to Legates and Willmott (1990) climatology. Accounting for soil freezing processes leads to more realistic present-day air temperatures in some areas: winter biases are reduced by up to 2 K in Northwestern Canada, and to a lesser extent, in Siberia, whereas in summer, the biases are also reduced in Eastern and Central Siberia. Note that the cooling effect in Northwestern Canada is not a direct thermal

impact of soil freezing but is attributed to changes in the atmospheric circulation. However, some biases are unaffected: air temperatures are still overestimated in winter over the Hudson Bay region and Southern Russia and, they are still slightly underestimated in summer over Alaska, Scandinavia and between 50°N–60°N in Russia. A large cold bias (−10 K) appears over the Kamchatka peninsula in both PD-F and PD-NF simulations.

Figure 9 shows that errors in summer precipitation are reduced over all Siberia in the PD-F experiment (between +1 and +1.5 mm day^{-1}) compared to more than +2 mm day^{-1} in the PD-NF simulation. Winter precipitation biases are not really modified when accounting for soil freezing. But the PD-F experiment still overestimates the rate of precipitation for most boreal regions during winter and summer.

The hydrological effect of soil freezing on present-day soil hydrology induces a strong soil dryness during summertime. To demonstrate that this effect is realistic, Fig. 10 compares the simulated soil moisture in PD-NF and PD-F experiments to selected ISLSCP data (Meeson et al. 1995) (volume 2) in the three studied regions (North America, Central and Eastern Siberia). Soil moisture from ISLSCP data is the average of the surface soil moisture and the deep soil moisture (at 50 cm depth). The seasonal cycle is improved and absolute values are much closer to the data when accounting for soil freezing in all regions. As a higher snow cover in North America than in Eurasia explained the different effects of soil freezing on present-day winter surface temperatures in these regions, simulated snow cover is compared to some NSIDC data (National Snow and Ice Data Center 1998) on Fig. 11. The annual evolution of snow cover extent, as simulated in PD-F and PD-NF experiments and monthly averaged over the years 1971–1995 by the NSIDC, is represented in North America and all Eurasia (30°E–180°E; 50°N–80°N). The model is able to simulate the maximum extent in winter with values very close to the observations both in North America and Eurasia. Nevertheless, summertime seems to be shorter in the model than in the NSIDC data, especially in Eurasia where the melting starts earlier in June and snowfall begins after September. No difference is indicated between the two curves of snow extent in PD-F and PD-NF simulations. As expected, soil freezing does not impact on the snow cover whereas snow cover does impact on the freezing and thawing processes.

Finally, simulated river discharges for the basins of Ob, Lena and Yenisei (Russia) have been compared to the R-ArcticNET dataset (Lammers et al. 2000). 10-year (1984–1994 for Ob and Lena, and 1985–1995 for Yenisei) of the observed monthly discharge rates have been calculated for each basin. The onset of the summer discharge maximum simulated in AGCM LMDz3.3 occurs 1 or 2 months too early. This is, at least in part, due to the fact that runoff from the southern parts of the basins, where snowmelt first occurs, is immediately

Fig. 7 Differences in winter mean sea level pressure (Pa) between PD-F and PD-NF experiments. *Dashed lines* means negative values
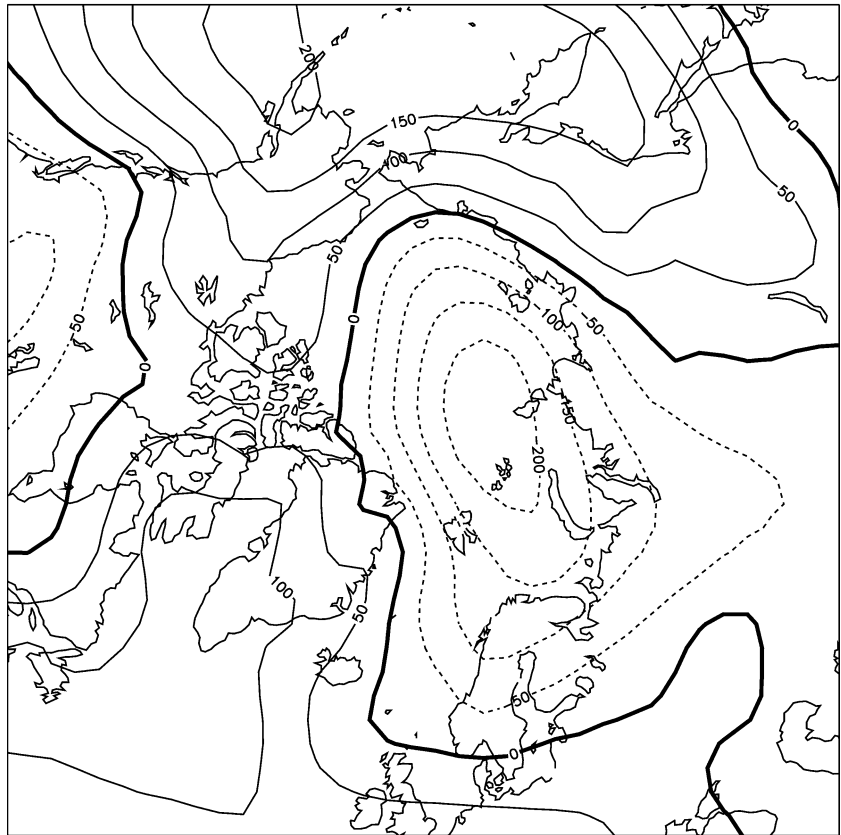

Fig. 8 Errors in simulated mean present-day 2 m air temperatures (K) with (*below*) and without (*above*) the inclusion of soil freezing relative to the Legates and Willmott (1990) climatology. Errors are represented for winter and summer
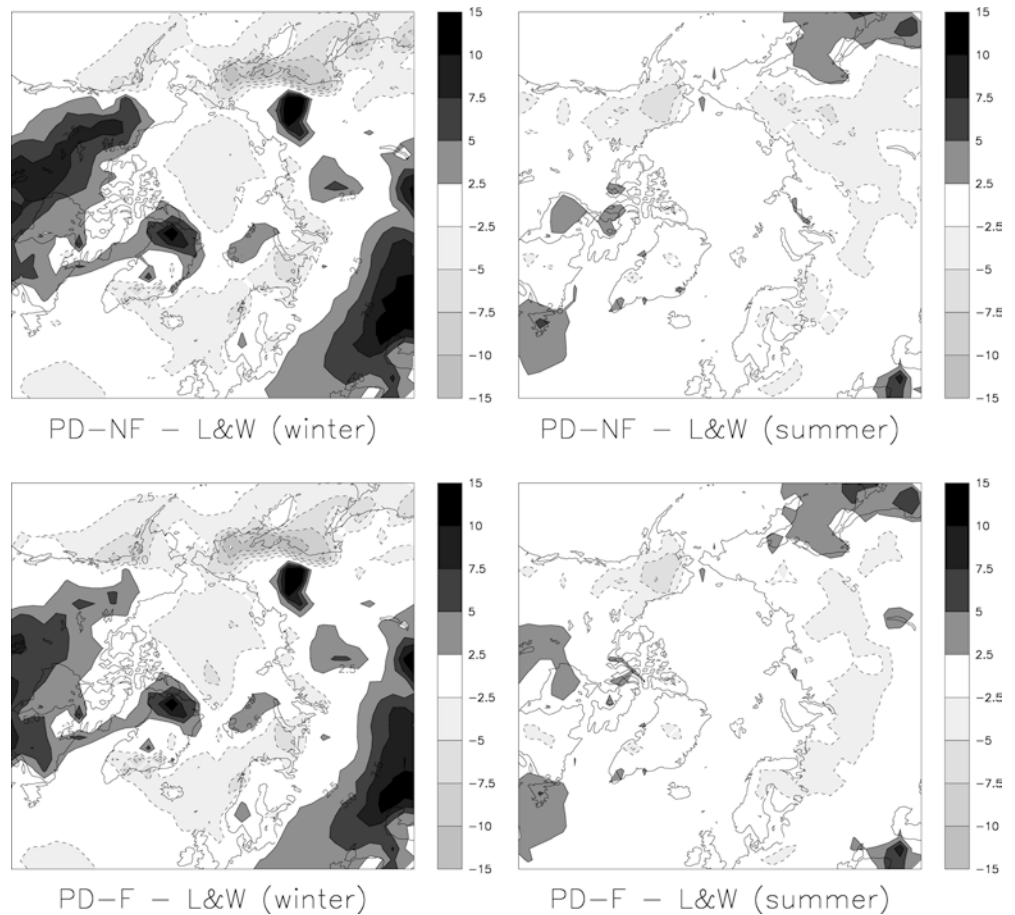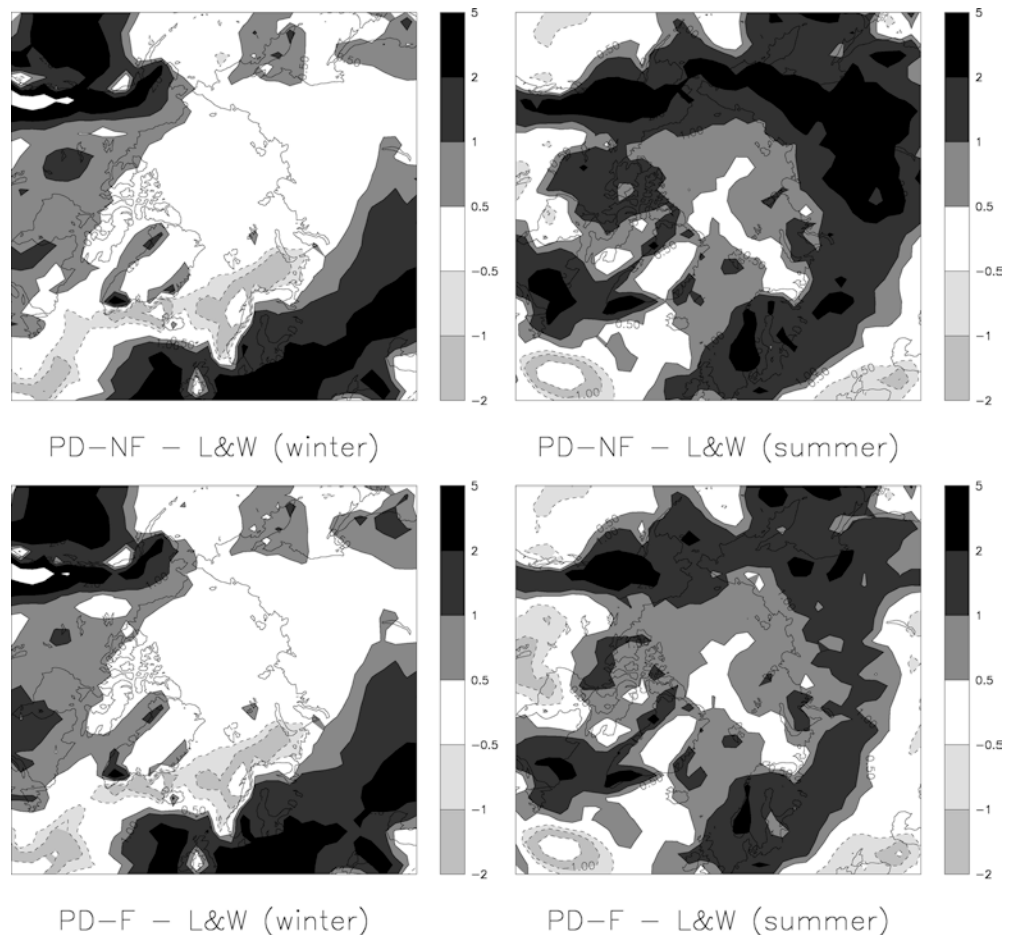
Fig. 9 Errors in simulated
mean present-day precipitation
(mm day^{-1}) with (*below*) and
without (*above*) the inclusion of
soil freezing relative to the
Legates and Willmott (1990)
climatology. Errors are
represented both for winter and
summer

PD−NF − L&W (winter)

PD−NF − L&W (summer)

PD−F − L&W (winter)

PD−F − L&W (summer)

considered to be lost to the ocean because there is no
surface water routing in the model. If we consider a
reasonable delay for routing water before it is lost to the
sea (for example, for the Yenisei river we supposed it
takes about 15 days to reach the Arctic ocean with a
1.5 m s^{-1} flow), the difference in discharge maximal is
reduced to 1 month. The seasonal cycle of Yenisei
discharge (Fig. 12) is improved when soil freezing is
accounted for. For the Lena river, no significant changes
on the seasonal cycle have been simulated by LMDz3.3
between the PD-F and PD-NF experiments. In the case
of the Ob, the simulated seasonal cycle in both present-
day experiments does not correspond to the observed
seasonal cycle. This disagreement might be explained by
the high wetland fraction that does exist in this region
and that have not been included in the model. Indeed,
wetlands play an important role in the surface hydrology
by intercepting melting water at spring. Therefore, the
surface runoff is reduced and the maximum of runoff is
delayed after springtime.

   These comparisons indicate that accounting for soil
freezing in the AGCM LMDz3.3 leads to some
improvements in the present-day simulated climate
(particularly on simulated surface hydrology), and that
at least, it does not induce larger biases compared to
observations.

4.3 Representation of permafrost areas

This section compares the permafrost and ground-ice
distributions estimated with the new surface scheme of
LMDz3.3 to available observations and recent statistics.
Two different methods were applied to the soil temper-
atures derived from the PD-F experiment to estimate
present-day permafrost distribution. The first one (and
the simplest one) consists in gathering the zones where
the maximum ground temperature at the deepest model
layer (at about 15 m depth) remains below 0°C. This
results in 27.8×10^6 km^2 of permafrost zones. The ob-
served total (continuous and discontinuous) permafrost
area, based on the IPA map (http://www.nsidc.com/
fgdc/maps/ipa_browse.html) (CAPS CD-ROM IPA
International Permafrost Association 1998) and the IPA
permafrost classification method using continuity (ex-
tent) and ground ice content, is about 22.8×10^6 km^2
(Zhang et al. 1999). Another estimate by Brown and
Haggerty (1998) gives 23.4×10^6 km^2 of total permafrost
areas, excluding glaciers and ice-sheets. Permafrost ex-
tent from PD-F experiment is respectively +22 and
+19% above these two studies. Figure 13a represents
the permafrost extent estimated with the simple method.
Compared to the IPA map, larger extents are simulated
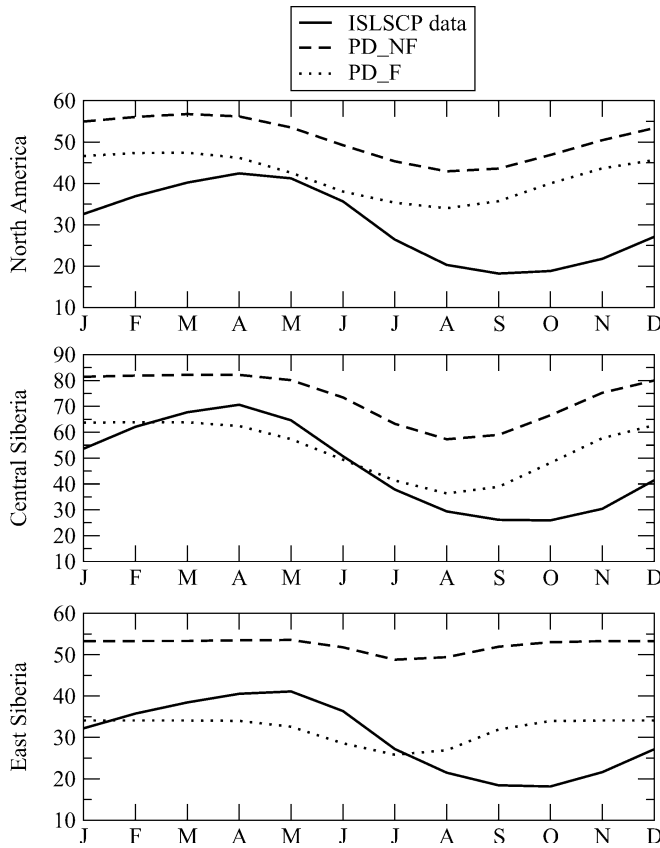at the East of Canadian Rockies and in western Baikal

Fig. 10 Comparison between simulated soil moisture (%) in PD-NF and PD-F experiments, and selected soil moisture ISLSCP data (Meeson et al. 1995). Data were available for the years 1987 and 1988

lake. Elsewhere, in Alaska, North Canada, North Siberia and over the Tibetan Plateau, permafrost areas are well reproduced. Note that larger permafrost estimates can be linked to cold biases during summertime,

previously mentioned over Alaska and the south part of Siberia.

The second approach is based on the "permafrost severity index", used by Anisimov and Nelson (1997) and Demchenko et al. (2001). This dimensionless number I is computed as

$$I = \frac{T_{\text{January}}}{T_{\text{July}}} \qquad (6)$$

where T represents the monthly mean surface air temperature in celsius degrees. Threshold values delimit the boundaries of the continuous/discontinuous permafrost. This calculation applied to simulated air surface temperatures (PD-F) yields different types of contemporary permafrost (Fig. 13b): total permafrost underlies 27.7×10^6 km^2 and continuous permafrost underlies 17.2×10^6 km^2. Absolute values for total permafrost are quite close to those of Demchenko et al. (2001). These authors reported 25.7×10^6 km^2 for total permafrost areas, with 12.7×10^6 km^2 for continuous zones when using results coming from the ECHAM4/OPYC3 experiment. But, permafrost zones are again overestimated compared to the IPA map and to Zhang et al. (1999). The largest differences occur for the continuous permafrost. Compared to the IPA map, Fig. 13b displays more continuous areas in the Ural region, in Central Alaska whereas the South and South West of the Hudson Bay show a deficit in permafrost areas. Overestimates of continuous zones by LMDz3.3 can also be here related to the cold summer bias mentioned in Sect. 4.2 which affects the Ural chains and strongly Central Alaska (see summer air temperatures on Fig. 8).

Despite the differences in absolute values, latitudinal extents of permafrost reproduced by LMDz3.3 (using both methods) have shown a good agreement with the study of Zhang et al. (1999). Therefore, general patterns

Fig. 11a, b Seasonal variations of snow cover extent (km^2) in PD-NF experiment (*dashed line*), in PD-F experiments (*plain line*) and according to data from the National Snow and Ice Data Center. Comparisons cover North America (165–55°W; 50–80°N) (**a**) and Eurasia (30–180°E; 50–80°N) (**b**)
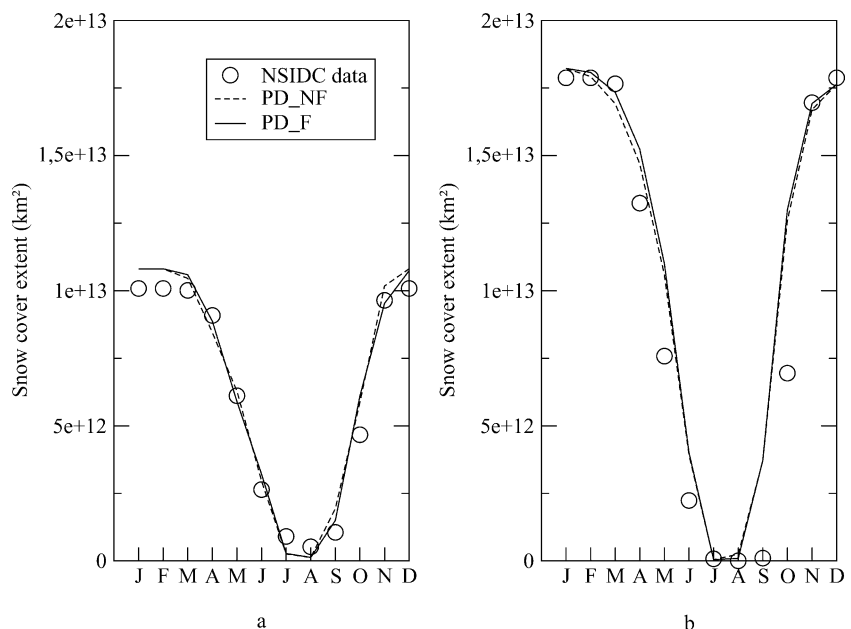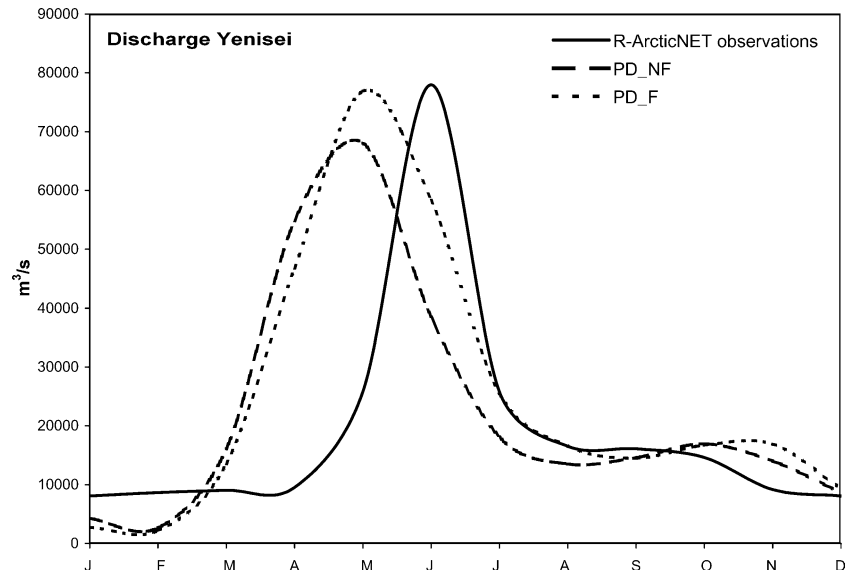
Fig. 12 Monthly Yenisei river discharge (m³ s⁻¹) as measured at the station Igarka (67.43°N; 86.48°E) over the period 1985–1995 (Lammers et al. 2000) and estimated in PD-NF and PD-F experiments

of permafrost distribution are well captured by the model.

5 AGCM results for future climate

5.1 Impact of soil freezing on future climate

The warming simulated by LMDz3.3, when soil water phase changes are taken into account, for the end of the twenty-first century, is (annual mean) between + 5 and + 9°C over boreal lands, which is in the range of other

models predictions (Anisimov et al. 2001). As commonly observed in $2\times CO_2$ simulated climate conditions, the warming is larger in winter than in summer.

5.1.1 Soil hydrology

In future climate conditions, soil freezing reduces mean annual soil moisture in North-western Canada, Eastern Siberia and around lake Baikal. Summer changes are illustrated on Fig. 14. These are also the regions where a maximum of dryness has been highlighted in present-day conditions. No significant changes are seen elsewhere.
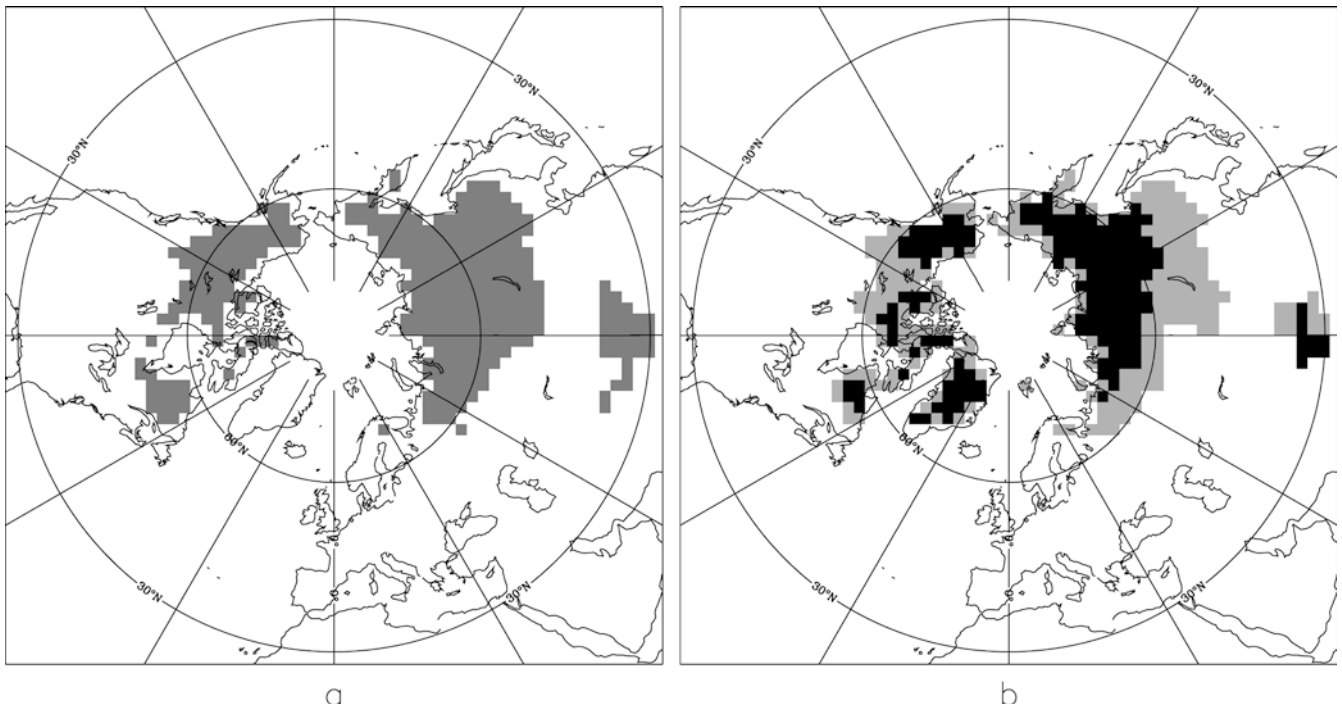

Fig. 13a, b Representation of permafrost areas in the PD-F experiment, calculated with the two methods: a simple one **a** and using the "severity index" **b** with the distinction of continuous zones in *black* and sporadic zones in *grey*

Soil freezing also induces reduced precipitation over all boreal lands, as in present-day climate, with maximal decrease in the same regions (North-West Canada, Eastern Siberia and around the Baikal lake) during summertime (Fig. 14). Nevertheless, this drying effect of soil freezing in a warmer climate is weaker (for example, between -5 and -10% in Siberia) than in PD-F experiment (around -15% in Siberia) owing to reduced frozen ground zones. Maximum decrease of precipitation is linked to decreased soil moisture and occurs in summer as well. One exception is again the Central-North Siberia (including the Ural region) where precipitation displays no change, in agreement with no significant soil moisture changes in this region.
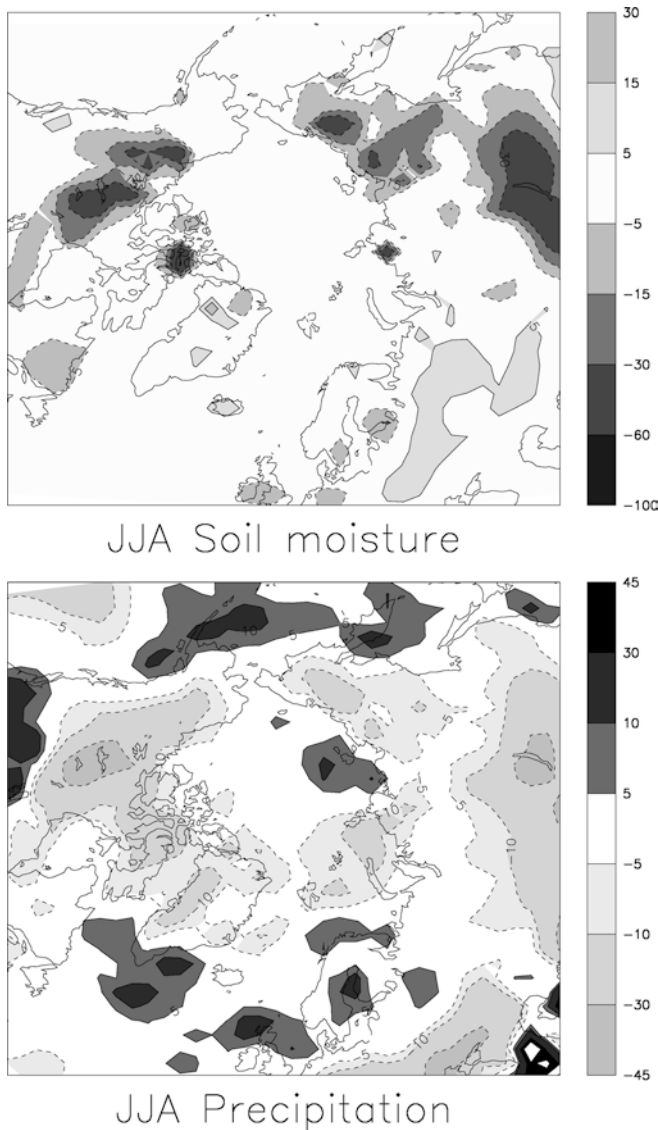

Fig. 14 Changes in summer soil moisture and precipitation induced by soil freezing under warmer conditions. Soil moisture differences between $2\times CO_2$-F and $2\times CO_2$-NF experiments are given in percent. Differences in precipitation are in percent relative to the $2\times CO_2$-NF run

5.1.2 Soil surface temperatures

Contrary to present-day conditions, thawing/freezing periods and absorption/release of associated latent heat essentially explain variations in $2\times CO_2$ surface temperatures.

Freezing period As mentioned in Sect. 4.1.2, the presence of snow cover during autumn can delay freezing in some specific regions and thus the associated heat release. Under $2\times CO_2$ conditions, snow cover is reduced compared to present-day snow cover (Fig. 6) and does not impact as much as in present-day climate on the formation of frozen ground. Figure 15 shows a global increase over boreal lands in surface temperatures during winter, and to a lesser extent, in autumn. This pattern is very well related to changes in sea level pressure. Indeed, an advection of warm air coming from southerly regions both over Siberia and North America (not shown) have been observed. Soil freezing is directly governed by air temperatures: it starts first in Eastern Siberia, the coldest region (about 20 days earlier in September compared to the other regions) and is extending to the whole boreal regions during winter. Therefore, contrary to present-day climate soil freezing strongly warms future winter surface temperatures. This effect may accelerate the disappearance of frozen ground areas and then could damage boreal ecosystems.

Thawing period Figure 15 displays a slight surface cooling effect induced in $2\times CO_2$-F experiment, well extended over Central and Eastern Siberia, from March to the end of summer. Under warmer conditions, thawing starts earlier in spring and continues to cool the surface during the first days of summertime in Siberia. It starts at mid April in Eastern Siberia (15 days earlier), at the end of March in Central Siberia (20 days earlier) and during the first 10 days of March in North America (15 days earlier). Furthermore, the snow cover in $2\times CO_2$-F experiment is less reduced in Eastern Siberia, the mean maximal height being 70 cm water equivalent, compared to 50 cm in Central Siberia and 30 cm in North America (see Fig. 6). In spring, soil thawing starts in these two latter regions whereas there is still some snow to melt in Eastern Siberia. Therefore, frozen ground will stay longer there and some of the melting processes are still visible in the beginning of summer where it provokes reduced surface temperatures compared to $2\times CO_2$-NF. In other regions, like in the Great Lakes Region, the near surface soil starts to warm once it completely thawed, leading to up to $+2$ K compared to $2\times CO_2$-NF.

During present-\day summertime, once snow and frozen ground have disappeared at the surface, the soil is systematically dryer in simulations that takes account for soil freezing, since the runoff water has been lost into the seas instead of infiltrating the soil. Under $2\times CO_2$

conditions, this effect is strongly attenuated because of less frozen ground, and cooler surface temperatures are observed on Fig. 15 when soil freezing is included.

On Fig. 14, small differences are simulated on precipitation rates and soil moisture between $2\times CO_2$-F and $2\times CO_2$-NF compared to those between PD-F and PD-NF. As soil freezing is less severe in $2\times CO_2$-F than in PD-F, it leads to a weaker impact on the soil water content and, therefore, the soil is not getting dryer during summertime as much as it gets under present-day conditions.

5.2 Future permafrost changes

5.2.1 Permafrost extent

The aim of this part is not to give an exact prediction of $2\times CO_2$ permafrost distributions for a given future date, but to show probable regional patterns of permafrost changes. Future distribution of permafrost areas has been diagnosed with the "permafrost severity index", applied to surface air temperatures of the $2\times CO_2$-F experiment. Sporadic permafrost is reduced around the

Baikal lake, over North America, the Ural chains and the Tibetan plateau. Greenland is less affected since only permafrost zones in the south are reduced. Table 2 quantifies these results and gives the estimates realized by Demchenko et al. (2001) for present-day, 2050 and 2100 years. Both studies predict one-third retreat of total permafrost zones in 2100, with a disappearance of more than half of the continuous zones. Whereas a larger retreat of total permafrost zones is evaluated in our study (-44%), continuous areas seem to be less affected than in Demchenko et al. (2001).

Besides, a regional comparison has been realized with the study conducted by Jin et al. (2000) on the Qinghai Tibet Plateau for permafrost predictions in 2009, 2049 and 2099, using an "altitude model" which diagnoses the lower limit as the mere criterion of permafrost distribution. For the next 100 years, the authors forecast a permafrost degradation between -8% (2009), -18% (2049) and -58% (2099) which corresponds respectively to an annual mean (simulated) surface air temperature increase of $+0.5°C$, $+1.1°C$ and $+2.9°C$. We roughly estimate a -35% reduction of permafrost areas over the same region for a temperature increase of $+4.4°C$. Although the predicted increase in temperature is higher in
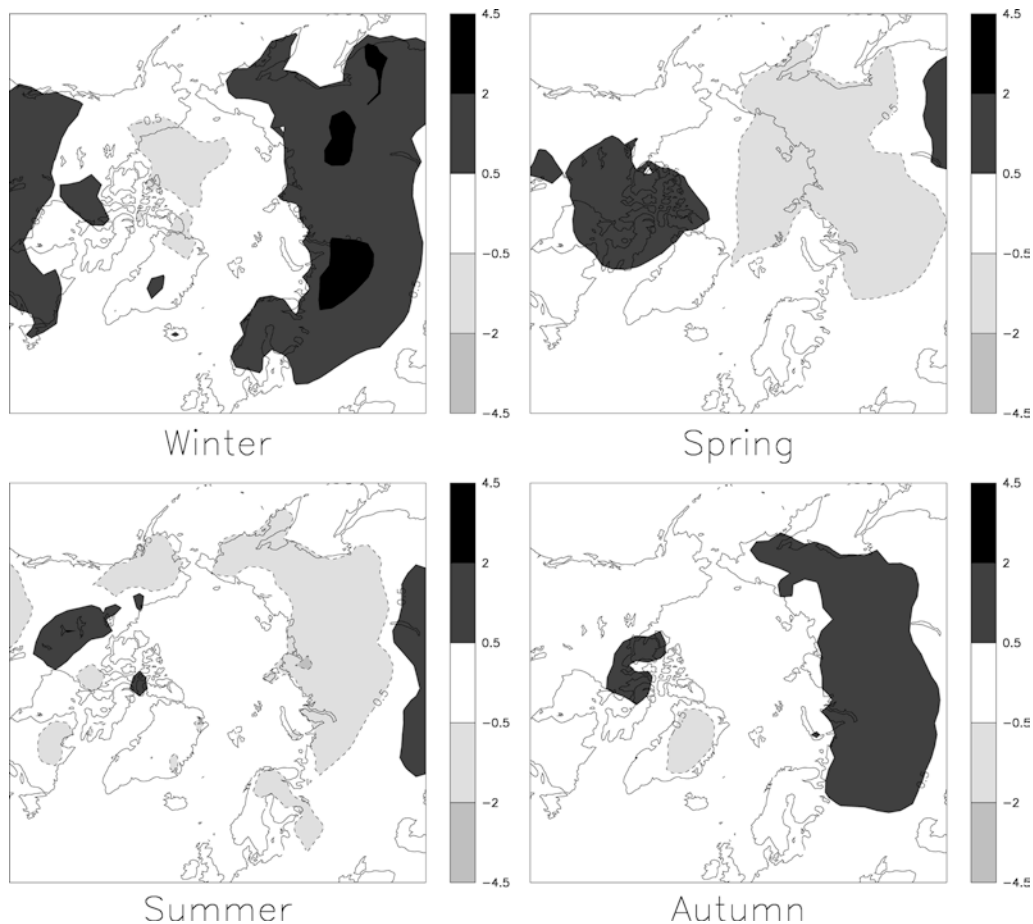

Fig. 15 Differences in seasonal mean surface temperatures (K) between $2\times CO_2$-F and $2\times CO_2$-NF experiments

Table 2 Comparisons of permafrost extent in millions of square kilometer between the study of Demchenko et al. (2001) using ECHAM4/OPYC3 simulations and $2\times CO_2$-F experiment

	Total permafrost cover			Continuous permafrost cover		
	PD	2050	2100	PD	2050	2100
ECHAM4/OPYC3	25.7	20−22%	17−18−34%	12.7	6−7−53%	2.5−3−80%
LMDz3.3	27.7		15.4−44%	17.2		7.9−54%

Percentages indicate the reduction of the areas relative to PD extents

LMDz3.3 than in the Jin et al. (2000) approach, permafrost extent is less reduced. However, both studies agree with a more important retreat in the Eastern and Southern Qinghai Tibet Plateau and on peripheral mountains, than in the interior of the Plateau. This prediction is coherent with the expected severe retreat of permafrost zones in the future in all contemporary southerly permafrost areas given by Anisimov and Nelson (1997): remaining equilibrium permafrost zones would be confined to Central Alaska, above the Hudson Bay, Eastern and Central Siberia, and the center of the Tibetan Plateau.

5.2.2 The active layer thickness

The thickness of the active layer, the layer of the soil between the atmosphere and permafrost subject to freezing and thawing on an annual basis, is an extremely important factor in polar ecology. Because most exchanges of energy, moisture, and gases between the atmosphere and terrestrial systems occur through it, changes in the thickness of the active layer could have serious impacts on geomorphical, hydrological and biological processes. According to the soil temperature profiles obtained in $2\times CO_2$-F and PD-F experiments, the active layer depth could increase by $+30\%$ in warmer conditions. By the way, Anisimov et al. (1997) used outputs from simulations carried on with the ECHAM1 A model (Cubash et al. 1992) and reported an increase of the active layer thickness of about $+10$ to $+20\%$. In both studies, largest relative increases are concentrated in the Russian Far East and in Alaska (not shown). Of course these two approaches do not account for changes in vegetation, which may result from warming and which could modify the soil response. However, all these projected changes in permafrost areas and active layer depths may generate different patterns of the sensitivity

of climate change to soil freezing at high latitudes since the soil column (thawed or frozen) would then respond differently.

6 Sensitivity of climate change to soil freezing

6.1 Temperatures changes

The possible sensitivity of temperature change to soil freezing is evaluated through the expression:

$$\Delta T_{\text{sens}} = (T_{2\times CO_2 \text{ - F}} - T_{\text{PD - F}}) \\ - (T_{2\times CO_2 \text{ - NF}} - T_{\text{PD - NF}}) \qquad (7)$$

or also

$$\Delta T_{\text{sens}} = (T_{2\times CO_2 \text{ - F}} - T_{2\times CO_2 \text{ - NF}}) \\ - (T_{\text{PD - F}} - T_{\text{PD - NF}}) \qquad (8)$$

Table 3 summarised the main positive or negative temperature effects induced by soil freezing on warming at high latitudes on the three studied regions: North America, Central Siberia and Eastern Siberia.

Soil freezing reduces the annual mean temperature increase only over Eastern Siberia (23% compared to the increase in surface temperatures expected without accounting for soil freezing). In the other boreal regions, soil freezing seems to enhance the future temperature increase $(T_{2\times CO_2 \text{ - NF}} - T_{\text{PD - NF}})$: by upto $+15\%$ in North America and by up to $+36\%$ in Central Siberia. These regional oppositions on an annual mean may be understood when looking at the seasonal patterns on Fig. 16. This figure shows that the warming is consistently enhanced in winter and reduced in summer. As stated before, this is due to a more intense warming in $2\times CO_2$ climate induced by the thermal effect of soil freezing during wintertime than in present-day climate.

Table 3 Annual mean temperature changes evaluated with and without including soil water phase changes in the surface scheme of LMDz3.3, between future and present-day climate and the sensitivity ΔT_{sens} to this parameterization

	$T_{2\times CO_2 \text{ - NF}} - T_{\text{PD - NF}}$ (K)	$T_{2\times CO_2 \text{ - F}} - T_{\text{PD - F}}$ (K)	ΔT_{sens} (K)	Relative changes due to freezing (%)
North America	$+5$	$+5.75$	$+0.75$	$+15$
Central Siberia	$+3.5$	$+4.25$	$+1.25$	$+36$
Eastern Siberia	$+5.5$	$+4.25$	-1.25	-23

Firstly, the weakened annual warming in Eastern Siberia (which corresponds to a negative ΔT_{sens}) is mainly due to summertime patterns. In the PD-F simulation, soil freezing leads to dryer soil conditions in summer and therefore to warmer surface temperatures, well marked in Eastern Siberia. As stated before, soil freezing is less severe under future climate conditions due to higher surface temperatures in autumn and winter. Thus, the effect of soil freezing on soil hydrology is less pronounced, thermal effect of soil thawing dominates and therefore, $2\times CO_2$-F surface temperatures are not higher than $2\times CO_2$-NF surface temperatures (see Fig. 15). As a consequence, simulated $(T_{2\times CO_2-F} - T_{PD-F})$ summer warming in Eastern Siberia is strongly reduced when soil freezing is accounted for. Summertime ΔT_{sens} reached minimal values (-6 K) in this region.

Besides, North America and Central Siberia display a positive ΔT_{sens} in annual mean which is particularly pronounced during wintertime (Fig. 16). From the freezing period in autumn, simulated climate change is stronger when soil freezing is taken into account. On one hand, Central Siberia undergoes a stronger surface warming due to thermal effects induced by soil freezing process in $2\times CO_2$ than in present-day conditions both in autumn and winter. This results in a positive ΔT_{sens} all over Central Siberia in autumn and winter. On the other hand, during wintertime in North America soil freezing

provokes lower surface temperatures in present-day conditions (displayed on Fig. 4) whereas $2\times CO_2$ surface temperatures are increased in $2\times CO_2$-F simulation. Thus, future winter warming is there particularly strengthened when soil freezing is included.

In spring, Fig. 16 indicates an increase of the surface warming when soil freezing is accounted for, over two large zones in North America and in the Ob Basin. Over North America the cooling thermal effect due to thawing is less important in $2\times CO_2$ (-0.5 K) than in present-day climate (between -1 and -2.5 K, see Figs. 4 and 5). These differences induce a maximum increase of the warming by up $+1.5$ K in Canada at this season.

Finally, we can stress once again the large dissymmetry between ΔT_{sens} in Eastern Siberia and over the remaining boreal regions (already pointed out in future comparisons, Sect 5.1). During spring and summer times, ΔT_{sens} is systematically lower in Eastern Siberia than elsewhere (that means the future surface warming is systematically more attenuated in this region than elsewhere when soil freezing processes are included in the model): the largest differences appear during summertime with a ΔT_{sens} equal to -6 K in the very eastern part of Siberia, compared to roughly -2 K elsewhere. Snow cover which isolates the surface from solar radiation plays an important role. We have already observed that future snow cover reduction in Eastern Siberia is weak and that this difference is responsible both for a delay of

Fig. 16 Seasonal sensitivity of future surface temperature change to soil freezing (ΔT_{sens}) as simulated by LMDz3.3
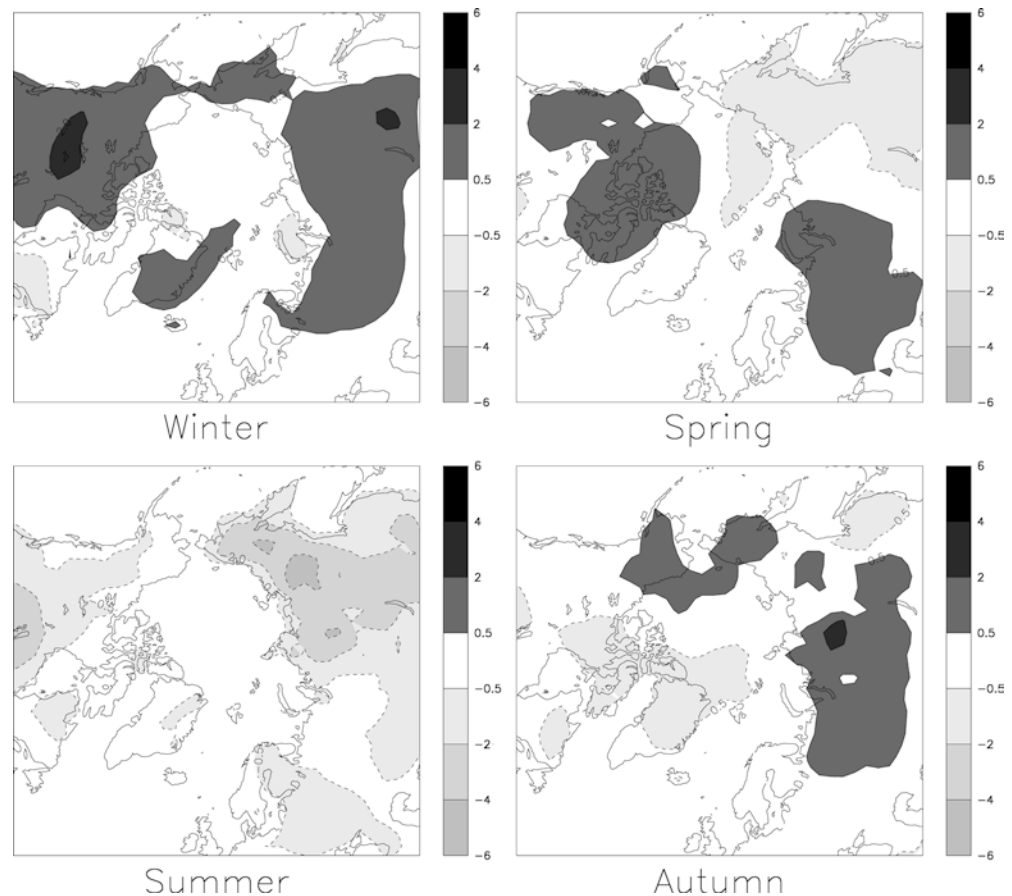
thawing there (which explains the negative ΔT_{sens} in spring and summer) and for a delay of freezing in autumn. The snow albedo can also be invoked: when snow melts, the surface albedo decreases, accelerating the warming of the surface and then the melting of snow and frozen grounds. This rapid surface warming in springtime has already been pointed out by Groisman et al. (1994) who showed that the global retreat of the spring snow cover over the last 20 years has enhanced the warming in the Northern Hemisphere. In this study, as stated before, the difference in future snow cover reduction between regions induces different rates of warming. This is a possible future scenario that can explain the enhancement of the increase of surface temperatures for the end of the twenty-first century in some regions (North America and Central Siberia) while other regions as in Eastern Siberia may undergo a reduced warming.

6.2 Hydrological changes

We analyse briefly in this final part the impact of soil freezing on precipitation changes, i.e. changes in precipitation between $2\times CO_2$ and present-day climates with and without including soil freezing process. The effect of soil freezing is to enhance the expected increase in future precipitation (May and Roeckner 2001) in all boreal lands. In annual mean, precipitation increases strongly over all Siberia (more than $+25\%$ in some places) and over the Great Lakes region when soil freezing is included. Maximal impact of soil freezing on precipitation changes occurs in summer. Indeed, at this season there is almost no influence on the difference of precipitation between future and present-day climate when soil freezing is excluded, whereas the increase reaches $+30\%$ when accounting for it. This is mainly due to the strong soil dryness discussed previously in Sect. 4.1 caused by soil freezing in summer under present-day conditions.

7 Conclusions

This study has demonstrated that the inclusion of soil freezing processes in a GCM can have a significant impact on simulated climate and on climate sensitivity to doubling atmospheric CO_2 in boreal regions. A simple soil scheme has been successfully incorporated into the LMDz3.3 AGCM. Four simulations have been carried out to analyse the potential impacts of soil freezing on modern and $2\times CO_2$ climate. To sum up, freezing acts to warm the high latitudes in winter and autumn (releasing of heat at the surface) while thawing at spring cools down the surface. But some specific and regional patterns must be considered for each period of time. In present-day climate summer becomes dryer when including soil freezing. Meltwater cannot infiltrate the soil (the remaining frozen soil) and is finally lost into the oceans, leading to a very low soil humidity

and then to warmer surface temperatures. $2\times CO_2$ climate is less affected by this hydrological effect induced by soil freezing because of less frozen ground areas. But thermal effects due to thawing and freezing are dominant, and particularly freezing is efficient in enhancing the expected future warming during wintertime. Furthermore regionally varying behaviours appear when considering the sensitivity of climate change to soil freezing. Combined patterns for changes in present-day and $2\times CO_2$ climate due to the inclusion of soil freezing yield an amplification of the future warming by up $+15\%$ in North America and $+36\%$ in Central Siberia. Only Eastern Siberia could undergo a reduced warming (-23%). Snow cover plays an important role in isolating the surface from solar radiation: it delays thawing at spring (so the surface is still cooling during summer) and delays freezing in autumn. Thus the different height of snow cover between East Siberia and the other regions in a $2\times CO_2$ climate is partly responsible for the different signs of the sensitivities of climate change.

We conclude that soil freezing does have a regional impact on the simulation of climate change. This work underlines the necessity of accounting for the locally dominant surface-atmosphere interactions (vegetation, soil freezing, snow cover, continental water) in climate models to perform valuable regional climate predictions.

References

Anisimov OA, Nelson FE (1997) Permafrost zonation and climate change in the Northern Hemisphere: results from transient general circulation models. Climatic Change 35:241–258

Anisimov OA, Shiklomanov NI, Nelson FE (1997) Global warming and active-layer thickness: results from transient general circulation models. Glob Planet Change 15:61–77

Anisimov O, Fitzharris B, Hagen JO, Marchant H, Nelson F, Prowse T, Vaughan DG (2001) Polar regions (Arctic and Antarctic). In: Houghton JT, Ding Y, Griggs DJ, Noguer M, Van der Linden PJ, Dai X, Maskell K, Johnson CA (eds) Climate change 2001: impacts, adaptation and vulnerability contribution of working group I to the third assessment report of the IPCC. Cambridge University Press, Cambridge

Bonan G (1996) A land surface model (LSM version 1.0) for ecological, hydrological, and atmospheric studies: technical description and user's guide. NCAR Technical Note 417, NCAR, Boulder Co., USA

Bonfils C, de Noblet-Ducoudré N, Braconnot P, Joussaume S (2001) Hot desert albedo and climate change: mid-Holocene monsoon in north Africa. J Climate 14:3724–3737

Boone A, Masson V, Meyers T, Noilhan J (2000) The influence of the inclusion of soil freezing on simulations by a soil-vegetation-atmosphere transfer scheme. J Appl Meteor 39:1544–1569

Bowling L, Lettenmaier D, Graham P, Clark D, El Maayar M, Essery R, Goers S, Gusev Y, Habets F, Van den Hurk B, Jin J, Kahan D, Lohmann D, Ma X, Mahanama S, Mocko D, Nasonova O, Niu G, Samuelson P, Shmakin A, Takata K, Verseghy D, Viterbo P, Xia Y, Xue Y, Yang Z (2003) Simulation of high-latitude hydrological processes in the Torne Kalix basin: PILPS phase 2(e) 1: experiment description and summary intercomparisons. Global Planet Change 38:1–30. DOI 10.1016/S0921-8181(03)00003-1

Brown J, Haggerty C (1998) Permafrost digital databases now available. EOS Trans Am Geophys Union 79:634

Cherkauer KA, Lettenmaier DP (1999) Hydrologic effects of frozen soils in the upper Mississippi river basin. J Geophys Res 104:19599–19610

Cox PM, Betts RA, Bunton CB, Essery RLH, Rowntree PR, Smith J (1999) The impact of a new land surface physics on the GCM simulation of climate and climate sensitivity. Clim Dyn 15:183–203

Cubasch U, Hasselmann K, Hock H, Maier-Reimer E, Mikolajewicz U, Santer BD, Sausen R (1992) Time-dependent greenhouse warming computations with a coupled ocean-atmosphere model. Clim Dyn 8:55–69

Demchenko PF, Eliseev AV, Mokhov II (2001) Sensitivity of permafrost cover in the Northern Hemisphere to climate change. Clivar Exchanges 6:9–11

Douville H, Royer JF (1996) Sensitivity of the Asian summer monsoon to an anomalous eurasian snow cover within the Météo-France GCM. Clim Dyn 12:449–466

Farouki OT (1981) The thermal properties of soils in cold regions. Cold Regions Sci Tech 5:67–75

Fox JD (1992) Incorporating freeze-thaw calculations into a water balance model. Water Resour Res 28:2229–2244

Fukuda M (1994) Methane flux from thawing siberian permafrost (ice complexes)-results from field observations. EOS Trans Am Geophys Union 75:86

Gel'fan AN (1989) Comparison of two methods of calculating soil freezing depth. Sov Meteor Hydrol 2:78–83

Goulden ML, Wofsy SC, Harden JW, Trumbore SE, Crill PM, Gower ST, Fries T, Daube BO, Fan SM, Sutton DJ, Bazzaz A, Munger JW (1998) Sensitivity of boreal carbon balance to soil thaw. Science 279:214–217

Groisman PY, Karl TR, Knight RW (1994) Observed impact of snow cover on the heat balance and the rise of continental spring temperatures. Science 263:198–200

Harzallah A, Sadourny R (1995) Internal versus SST-forced atmospheric variability as simulated by an atmospheric general circulation model. J Climate 8:474–495

Henderson-Sellers A, Yang ZL, Dickinson RE (1993) The project for intercomparison of land-surface parameterisation schemes. Bull Am Meteor Soc 74:1335–1349

Henderson-Sellers A, Pitman A, Love P, Irannejad P, Chen T (1995)) The project for intercomparison of land-surface parameterisation schemes (PILPS): phases 2 and 3. Bull Am Meteor Soc 76:489–503

International Permafrost Association Data Information Working Group (1998) In: National Snow and Ice Data Center (eds) digital data available from:nsidc@kryos.colorado.edu

Jin H, Li S, Cheng G (2000) Permafrost and climatic change in China. Glob Planet Change 26:387–404

Koren V, Schaake J, Mitchell K, Duan QY, Chen F, Baker JM (1999) A parameterization of snowpack and frozen ground intended for NCEP weather and climate models. J Geophys Res 104:19569–19586

Krinner G, Genthon C, Li Z-X, Le Van P (1997) Studies of the Antarctic climate with a stretched-grid general circulation model. J Geophys Res 102:13731–13745

Krinner G (2003) Impact of lakes and wetlands on boreal climate. J Geophys Res 108. DOI:10.1029/2002JD002597

Lammers RB, Shiklomanov AI (2000) R-arctinet, a regional hydrographic data network for the pan-arctic region. Published on CD National Snow and Ice Data Center

Legates DR, Willmott C (1990) Mean seasonal and spatial variability in gauge-corrected global precipitation. Int J Climatol 10:111–127

Lunardini V (1988) Heat conduction with freezing or thawing. Technical Report 88-1, US Army Corps of Engineers

Luo L, Robock A, Vinnikov K, Schlosser A, Slater A et al (2003) Effects of frozen soil temperature, spring infiltration, and runoff: results from the PILPS 2(d) experiment at Valdai, Russia. J Hydrometeorol 4:334–351

Matthews E, Fung I (1987) Methane emission from natural wetlands: global distribution, area, and environmental characteristics of sources. Glob Biogeochem Cyc 1:61–86

May W, Roeckner E (2001) A time slice experiment with the ECHAM4 AGCM at high resolution: the impact of horizontal resolution on annual mean climate change. Clim Dyn 17:407–420

Meeson BW, Corprew FE, McManus JMP, Myers DM, Closs JW, Sun KJ, Sunday DJ, Sellers PJ (1995) ISLSCP Initiative 1-Global data sets for land atmosphere model: 1987–1988. Published on CD by NASA available from http://daac.gsfc.nasa.gov/CAMPAIGN_DOCS/ISLSCP/islscp_i1.html

Michaelson GJ, Ming CL, Kimble JM (1996) Carbon storage and distribution in tundra soils of Arctic Alaska USA. Arct Alp Res 28:414–424

National Snow and Ice Data Center (1998) Northern Hemisphere weekly snow cover and sea ice extent. Digital data available from:nsidc@kryos.colorado.edu

Nelson FE, Anisimov OA (1993) Permafrost zonation in Russia under anthropogenic climatic change. Permafrost Periglacial Process 4:137–148

Prigent C, Matthews E, Aires P, Rossow W (2001) Remote sensing of global wetland dynamics with multiple satellite data sets. Geophys Res Lett 28:4631–4634

Renssen H, Isarin RFB, Vandenberghe J, Lautenschlager M, Schlese U (2000) Permafrost as a critical factor in paleoclimate modelling: the younger dryas case in Europe. Earth Planet Sci 176:1–5

Roeckner E, Arpe K, Bengtsson L, Christoph M, Claussen M, Dümenil L, Esch M, Giorgetta M, Schlese U, Schulzweida U (1996) The atmospheric general circulation model ECHAM-4: model description and simulation of present-day climate. MPI Report 218:90

Roeckner E, Bengtsson L, Feichter J (1999) Transient climate change simulations with a coupled atmosphere-ocean GCM including the tropospheric sulfur cycle. J Clim 12:3004–3032

Schlosser C, Robock A, Vinnikov K, Speranskaya A, Xue Y (1997) 18-year land-surface hydrology model simulations for a mid-latitude grassland catchment in Valdai, Russia. Monthly Weather Rev 125:3279–3296

Schlosser C, Slater AG, Robock A, Pitman AJ, Vinnikov KY, Henserson-Sellers A, Speranskaya NA, Mitchell K, Boone A, Braden H, Chen F, Cox P, de Rosnay P, Desborough CE, Dickinson RE, Dai YJ, Duan Q, Entin J, Etchevers P, Gedney N, Gusev YM, Habets F, Kim J, Koren V, Kowalczyk E, Nasonova ON, Noilhan J, Schaake J, Shmakin AB, Smirnova TG, Verseghy D, Wetzel P, Xue Y, Yang ZL (2000) Simulations of a boreal grassland hydrology at Valdai, Russia: PILPS phase 2(d). Monthly Weather Rev 128:301–321

Smirnova TG, Brown JM, Benjamin SG, Kim D (2000) Parameterization of cold-season processes in the MAPS land-surface scheme. J Geophys Res 105:4077–4086

Smith SL, Burgess MM (1999) Mapping the sensitivity of canadian permafrost to climate warming. In: Proceedings of IUGG 99 Symposium, vol 256. HS2 IAHS Publications, pp 71–80

Takata K, Kimoto M (2000) A numerical study on the impact of soil freezing on the continental-scale seasonal cycle. J Meteorol Soc Jpn 78:199–221

Vinnikov KY, Robock A, Speranskaya NA, Schlosser CA (1996) Scales of temporal and spatial variability of midlatitude soil moisture. J Geophys Res 101:7163–7174

Viterbo P, Beljaars ACM (1995) An improved land surface parameterization scheme in the ECMWF model and its validation. J Climate 8:2716–2748

Viterbo P, Beljaars ACM, Mahfouf JF, Teixeira J (1999) The representation of soil moisture freezing and its impact on the stable boundary layer. QJR Meteorol Soc 125:2401–2426

Waelbrock C (1993) Climate-soil processes in the presence of permafrost: a system modelling approach. Ecol Model 69:185–225

Weller G, Chapin FS, Everett KR, Hobbie JE, Kane D, Oechel WC, Ping CL, Reeburgh WS, Walker D, Walsh J (1995) The Arctic flux study: a regional view of trace gas release. J Biogeogr 22:365–374

Zhang T, Barry RG, Brown J (1999) Statistics and characteristics of permafrost distribution in the Northern Hemisphere. Polar Geogr 23:132–154